Supervised Classification of Metatranscriptomic Reads Reveals the Existence of Light-dark Oscillations During Infection of Phytoplankton by Viruses

Enzo Acerbi[1,*], Caroline Chenard[2,*], Stephan C. Schuster[1] and Federico M. Lauro[1,2]

[1]*Singapore Centre on Environmental Life Sciences Engineering (SCELSE), Nanyang Technological University, 60 Nanyang Dr, 637551, Singapore*

[2]*Asian School of the Environment, Nanyang Technological University, 50 Nanyang Avenue, 639798, Singapore*

[*] *These authors contributed equally.*

Keywords: Support Vector Machines, Empirical Mode Decomposition, Marine Microbial Ecology.

Abstract: In the era of next generation sequencing technologies microbial species identification is typically performed using sequence similarity and sequence phylogeny based approaches. Particularly challenging is the discrimination of closely related sequences such as auxiliary metabolic genes (AMGs) in cyanobacteria and their viruses (cyanophages). Here we developed a method which combines Support Vector Machine based classification of AMGs short fragments and Empirical Mode Decomposition of periodic features in time-series. We applied this method to investigate the transcriptional dynamics of viral infection in the ocean, using data extracted from a previously published metatranscriptome profile of a naturally occurring oceanic bacterial assemblage sampled Lagrangially over 3 days. We discovered the existence of light-dark oscillations in the expression patterns of AMGs in cyanophages which follow the harmonic diel transcription of both oxygenic photoautotrophic and heterotrophic members of the community. These findings suggest that viral infection might provide the link between light-dark oscillations of microbial populations in the North Pacific Subtropical Gyre.

SCIENCE AND TECHNOLOGY PUBLICATIONS

1 INTRODUCTION

Like most of life sciences, marine microbial ecology has also been revolutionized by the advent of next generation sequencing (NGS) technologies. Taxonomical identification of DNA/RNA sequences (also referred to as fragments) is typically performed by checking for the existence of a similarity by alignment to the genomes of all the known microbial species in a brute force kind of fashion. If matches are found, phylogenetic analysis may subsequently be conducted to unravel the evolutionary relationships among the species. This similarity based identification approach has two main limitations: Firstly, the extensive number of comparison to be performed makes the task computationally expensive, which translate in high costs and long processing time. Secondly, NGS technologies can generate sequences of limited length (typically 250 bp). While this may not represent an issue with distantly related sequences, it can make the discrimination of closely related sequences (high similarity) difficult. This is the case for auxiliary metabolic genes (AMGs) in cyanobacteria and their associated viruses (also referred to as cyanophages). AMGs are encoding key metabolic functions such as photosynthesis, carbon metabolism, etc. Upon infection, viruses take over the control of the bacterial cell and keep it alive expressing the AMGs that they are carrying, for which an high similarity with the bacterial AMGs is required for a successful infection.

Being able to determine whether an AMG short fragment (fragments that does not cover the entire length of the AMG) belongs to a bacterial host or its associated viruses is an extremely valuable resource in microbial ecology. In the past, alternative methods exploiting specific genetic content have been used to characterize the origin of a gene (Sandberg et al., 2001). Recently, Tzahor *et al.* (Tzahor et al., 2009) used a multi-class Support Vector Machine (SVM) to rapidly classify core-photosystem-II gene and transcripts fragments coming from marine samples based on their oligonucleotide frequencies. Here, we applied a SVM-based approach to classify short fragments of two diffent AMGs, na-

Acerbi, E., Chenard, C., Schuster, S. and Lauro, F.
Supervised Classification of Metatranscriptomic Reads Reveals the Existence of Light-dark Oscillations During Infection of Phytoplankton by Viruses.
DOI: 10.5220/0006763200690077
In *Proceedings of the 11th International Joint Conference on Biomedical Engineering Systems and Technologies (BIOSTEC 2018) - Volume 3: BIOINFORMATICS*, pages 69-77
ISBN: 978-989-758-280-6
Copyright © 2018 by SCITEPRESS – Science and Technology Publications, Lda. All rights reserved

mely *psbA* and *phoH*, retrieved from a previously published metatranscriptome profiling of multiple naturally occurring oceanic bacterial populations sampled in situ over 3 days (Ottesen et al., 2014). The short *psbA* and *phoH* fragments (with length ranging between 150 and 300bp) were classified based on their origin (viral vs host) using GC content, mono-, di-, tri-, tetra-nucleotide frequencies as discriminating features.

The outputs were further processed using Empirical Mode Decomposition (EMD) to identify the underlying frequency dynamics of transcription during viral infection in environmental cyanobacterial populations. EMD can deconvolve natural time-series data into composing frequencies also known as intrinsic mode functions (IMFs). EMD has been used successfully to analyse time series data in other scientific domains including the detection of periodically expressed genes in microarray data (Chen et al., 2014), analysis of seismic data (Han and van der Baan, 2013), electrocardiograms (Chang, 2010) and anomaly in sea-surface height (Li et al., 2012). Our data demonstrated an existence of light-dark oscillation in the expression pattern of AMGs in cyanophages suggesting that viral infection patterns might provide the dynamic coupling between light-dark oscillations of autotropic and heterotrophic microbial populations in the North Pacific Subtropical Gyre.

2 BIOLOGICAL BACKGROUND

Marine picocyanobacteria from the genera *Synechococcus* and *Prochlorococcus* are major primary producers in the ocean at low- and mid-latitude and contribute significantly to the global carbon cycle (Hess, 2004; Partensky et al., 1999). Given that light represents the main source of energy for cyanobacteria, it also determines the tempo of carbon fixation, metabolic and physiological activity such as the timing of cell division, amino acid uptake, nitrogen fixation, photosynthesis and respiration (Ni and Zeng, 2016; Golden et al., 1997). For example, nearly half of all *Prochlorococcus* population in the North Pacific Subtropical Gyre demonstrated a transcriptional diel cycle (Ottesen et al., 2014). Viral infection in the oceans might also be synchronized with the light cycle. Some studies suggest a diel cycle in the number of infective viruses which could mainly be attributed to UV damage during the peak of sunlight (Wilhelm et al., 1998; Suttle and Chen, 1992). However, the timing of viral replication can also be influenced by the presence and absence of light. For example, a temporal study at a station in the Indian Ocean revealed a strong increase in viral abundance in the middle of the night (Clokie et al., 2006a). Logically, the synchronicity between light and replication is especially important for viruses infecting cyanobacteria, the cyanophages. Indeed, it was shown that light influences viral fitness as light is required for viral infection as it might influence the degradation of host genomic DNA, viral transcription or production of new progeny (Thompson et al., 2011).

In addition, cyanophages harbour AMGs which are usually homologs of host genes involved in photosynthesis and carbon metabolism pathways. These AMGs likely play a role in viral infection (Breitbart et al., 2007). For example, the *psbA* gene which encode D1 protein involved in the photosystem II (PSII) reaction centre is prevalent in cyanophage genomes. PSII is particularly sensitive to photodamage causing a high turnover rate for the D1 protein. It was shown that viral *psbA* can highly be transcribed during infection which suggests that viral-*psbA* expression might maintain the photosynthetic activity of the infected host cells and therefore provide energy for cyanophage replication (Clokie et al., 2006b; Lindell et al., 2007). This is supported by the notion that during the lytic cycle of infection of *Prochlorococcus* MED4 by cyanophage P-SSP7 most of the *psbA* transcript in infected cells were from viral origin after 6hrs (Lindell et al., 2007). Similarly, the *phoH* gene which is involved in phosphate metabolism was previously found in both heterotroph and autotroph phages (Goldsmith et al., 2011).

Based on sequence phylogeny, viral *psbA* can generally be distinguished from *Synechococcus* and *Prochlorococcus* (Sullivan et al., 2006; Chenard and Suttle, 2008), while *phoH* genes cluster together based on their origin (i.e. autotroph bacteria, heterotroph bacteria, cyanophage, heterotroph phage and eukaryotic viruses (Goldsmith et al., 2011; Goldsmith et al., 2015)).

3 METHODS

3.1 Support Vector Machines

Support Vector Machines (SVMs) are a supervised learning algorithm in machine learning, first introduced by Vapnik (Stitson et al., 1996) and based on the principle of structural risk minimization. Given labeled data (in our case, DNA fragment whose origin is known), a SVM can be trained to individuate the optimal hyperplane separating (classifying) new examples.

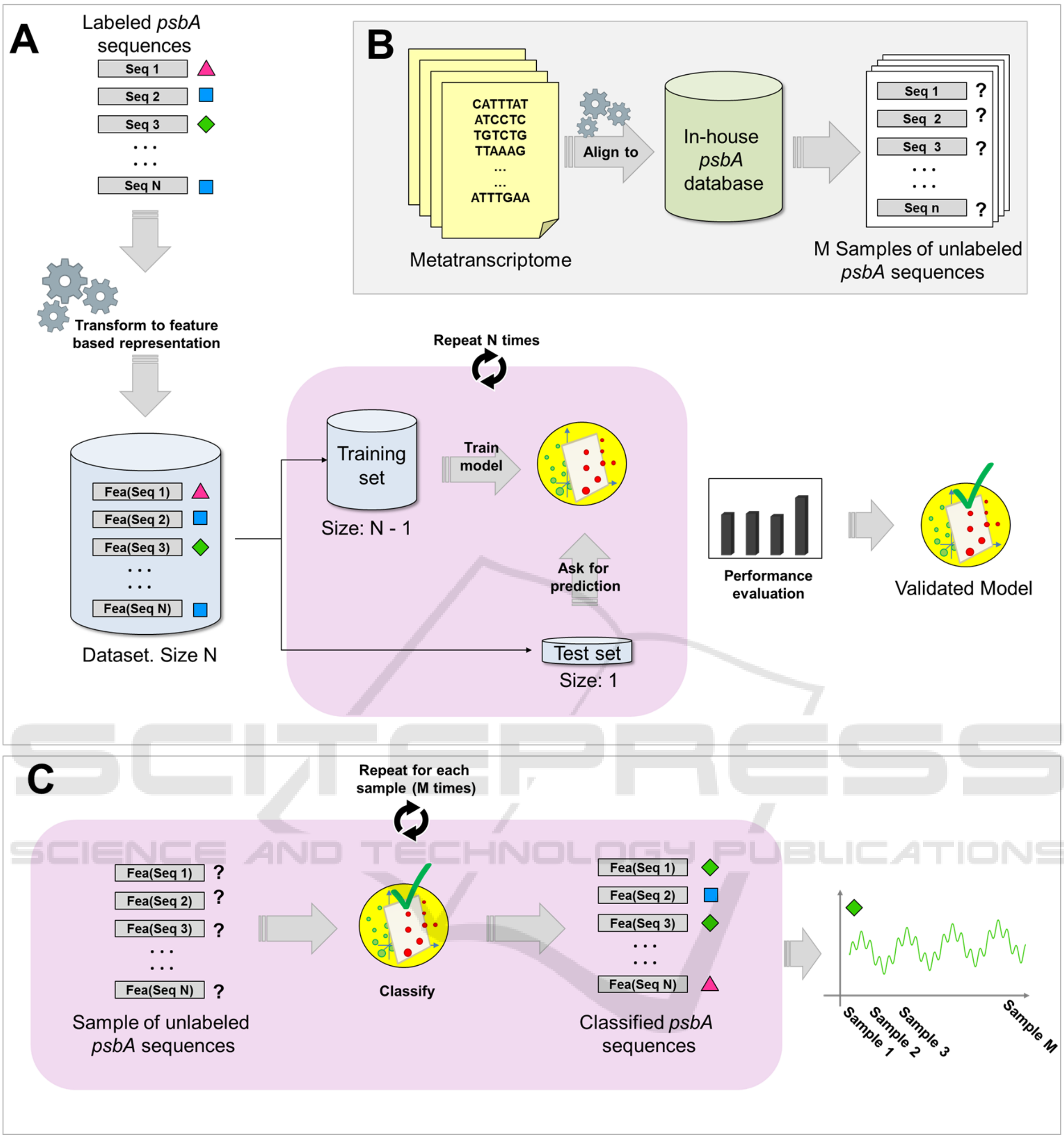

SCITEPRESS SCIENCE AND TECHNOLOGY PUBLICATIONS

Figure 1: (A) Training and validation of the SVM-based classifier (B) Extraction of *psbA* fragments from the metatranscriptome. (C) Classification of new sequences using the SVM-based classifier. The same procedure was performed for the *phoH* gene.

3.2 Training Set Generation

Labelled DNA sequences for *psbA* and *phoH* genes are scarce in the literature. In order to generate the *psbA* training set for the SVM-based multiclassificator, we collected 203 *psbA* DNA sequences from NCBI (including those used by Tzahor S. *et al.* (Tzahor et al., 2009)). Sequences in the dataset were labelled as belonging to one of the following five categories: *Synechococcus* bacteria (77), *Synechococcus* virus (42), *Prochlorococcus* bacteria high-light (38), *Prochlorococcus* bacteria low-light (26) and *Prochlorococcus* virus (20). Sequences were long, having different lengths ranging from 720bp to 1083bp, with a median of 1080bp. Analogously, *phoH* training set was created by collecting 84 DNA sequences from NCBI. Sequences in the dataset were labelled as belonging to one of the following five categories: Autotrophic host (i.e. cyanobacteria) (17), cyanophage (29), heterotrophic host (13), heterotrophic phage

(14), phytoeukaryotic virus (10). *PhoH* sequences were also long, having different lengths ranging from 603bp to 1770bp, with a median of 766.5 bp. In their work, Tzahor *et al.* trained the SVM classifier using full length *psbA* sequences and subsequently used it for classification of other full length *psbA* sequences (Tzahor *et al.* also tested their classifier on short *psbA* fragments, but only limited to binary classification). If the aim is to use the classifier on shorter *psbA* fragments, the approach of Tzahor *et al.* may not always give the best results. In fact, classification accuracy may be low if the training is performed on clean samples (*psbA* full genes, rather than fragments) and the real-world classification is performed on noisy samples (*psbA* fragments. i.e. sequences containing a part of the *psbA* gene and other base pairs not related to the *psbA* gene, as in metagenomic/metatranscriptiomic data). For this reason, *psbA* and *phoH* training sets were generated by randomly extracting sequences of length 300bp from the original sets. In addition, to deal with the original dataset being slightly unbalanced (not equal number of instances for each class) a combination of undersampling and oversampling was applied to both *psbA* and *phoH* sequences in order to obtain balanced training sets: 100 sequences for each of the five classes (total of 500 sequences) for *psbA* training set and 50 sequences for each of the five classes (total of 250 sequences) for *phoH* training set.

3.3 Feature Generation

GC, mono-, di-, tri-, tetra-nucleotide frequencies were calculated for each sequence of the training sets (for a total of 341 features per sequence) and used as input feature vector for the SVM classifiers. When including penta- and/or hexa-nucleotide frequencies, no significant improvements in prediction accuracy were observed (data not shown).

3.4 The SVM-based Model

Although through the document it will be referred to as SVM-based classifier, the model is composed by 5 different SVM one-against-all classifiers with linear kernel, each of them trained to separate one of the five taxonomical categories (positive class) from all the remaining ones (collapsed as negative class). Associated with the prediction on whether a given sequence belongs or not to the positive class for which it was trained, each classifier returns a numeric value representing the probability estimate of the prediction. For each new sequence, the classifier returning the prediction associated with the highest probability estimate is the one determining the category of the sequence.

3.5 Model Training, Parameter Optimization and Validation

The LIBSVM toolbox (v3.22) (Chang and Lin, 2011) for MATLAB was used for the experiments. The SVM-based classifier was trained using the 500 and 250 sequences of the *psbA* and *phoH* training sets respectively. In order to assess the ability of the model to correctly assign each sequence to the respective taxonomical category, a cross validation of type leave-one-out was performed. This validating procedure iterates over all of the N sequences of a training set, each time using N-1 sequences to train the classifier and 1 sequence as a test. Performances were assessed in terms of precision, recall and f-measure, which for binary classification are defined as follows:

$$precision = \frac{\text{true positive}}{\text{true positive + false positive}} \tag{1}$$

$$recall = \frac{\text{true positive}}{\text{true positive + false negative}} \tag{2}$$

$$F_1 = 2 \cdot \frac{precision \cdot recall}{precision + recall} \tag{3}$$

In statistics the recall is referred to as sensitivity and the precision as positive predicted value. For *psbA*, cross validation mean precision resulted to be equal to 0.95, mean recall 0.92 and mean F_1 0.93. In this phase, the optimal value for the parameter Cost (cost of misclassification) was empirically established as being equal to 8, while the optimal probability estimate cut-off resulted to be equal to 0.3 (resulting in 3.8% of the sequences being marked as unassigned). A direct comparison of the SVM-based classifier with the previous work of Tzahor *et al.* is not feasible as in their study, Tzahor *et al.* performed the multi-class classification using full length *psbA* sequences, while tests with short fragments (100, 200 and 300 bp) were limited to binary classification only. For *phoH*, the mean precision resulted to be equal to 0.98, mean recall 0.98 and mean F_1 0.98. No optimal probability estimate cut-off was applied for *phoH* sequences while the parameter cost was set to 8.

3.6 Classification of Sequences Extracted from the Metatranscriptiome

In order to extract *psbA* and *phoH* fragments from the metatranscriptome data of Ottesen *et al.*, we firstly

SCITEPRESS SCIENCE AND TECHNOLOGY PUBLICATIONS

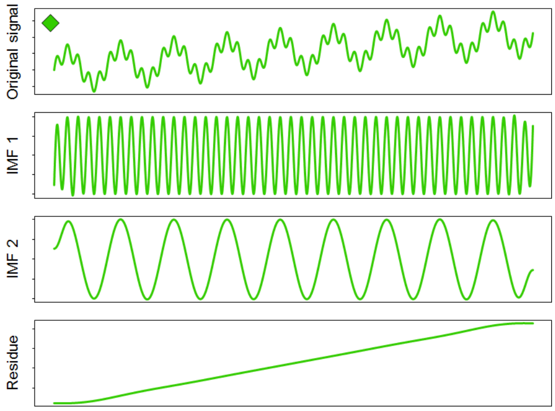

Figure 2: Example of Empirical Mode Decomposition of a simulated signal. Each IMF represents a different oscillatory component/frequency of the original signal and can be used to identify the different underlying processes that are responsible for generating the original signal. Oscillatory components are extracted in decreasing order of frequency.

built in-house *PsbA* and *PhoH* protein databases. The *PsbA* database was composed by 11,962 protein sequences retrieved from UniProtKB, while the *PhoH* database was composed by 100,501 protein sequences downloaded from NCBI. Subsequently, metatranscriptome data was screened for homology against these databases using Rapsearch2 (Zhao et al., 2011) (which allows protein similarity search by translating DNA/RNA queries into protein), retaining matches with alignment-length greater than 150 bp and e-value smaller than 0.000001 Figure 1B). For each time point, *psbA* and *phoH* fragments were then classified using the SVM-based classifier. Counts were normalized using the cumulative sum scaling (CSS) method (Paulson et al., 2013).

3.7 Empirical Mode Decomposition

Empirical mode decomposition (Huang et al., 1998), is a data-driven method for analysing of non linear and non stationary time frequency data, such as natural signals.

The EMD process iteratively decomposes the original signal into a finite number of intrinsic mode functions (IMF), that is, functions with a single mode/frequency 2. Each IMF represents a different component/frequency of the original signal and can be used to identify the different underlying processes that are responsible for generating the original signal (Figure 2). The EMD procedure works as follows: first, all the time series local minima and maxima are identified. Interpolation then is applied to connect the local minima among them, generating the lower envelope of the data. The same is performed on the local maxima, generating the upper envelope. Subsequently, the mean value of the envelope is calculated and subtracted from the original signal. This procedure takes the name of sifting and produces an IMF. To be considered valid, an IMF needs to satisfy the following conditions: (i) the number of extrema and of zero-crossings must differ by no more than one (ii) both lower and upper envelopes must have a mean equal to zero. The sifting procedure is repeated until no further IMF can be extracted from the original signal or the specified terminating criterion is met. IMFs are extracted in decreasing frequencies levels. EMD is a relatively recent approach that still holds some drawbacks. For instance, EMD may be prone to suffer from sampling errors as those could lead to incorrect placement of extema and therefore lead to inaccurate IMFs. Similarly, the usage of different interpolation methods can also lead to slight differences in the algorithm results, particularly in terms of flexibly and smoothness of the IMFs (Bagherzadeh and Sabzehparvar, 2015). IMFs are also challenging to interpret in absence of knowledge about the underlying system, and IMFs of different orders on different time series may not be capturing the same phenomena. In addition, analogous information may end up being contained in multiple IMFs and there can sometimes be lower-order IMFs that are just spurious fluctuations (which have the purpose of correct errors on other IMFs, so that they can sum up to the original signal) (Chambers, 2015). In this work EMD was run using the EMD R package (Kim and Oh, 2009), allowing a maximum number of sift iterations equal to 50, with a periodic type of boundary and constructing the envelops by interpolation. No meaningful changes in the results were observed when different boundaries and interpolation methods were tested.

4 RESULTS AND DISCUSSION

A total of 20,235 *psbA* and 5,008 *phoH* short sequences (length ranging from 150 to 300b) extracted from the high-resolution metatranscriptome time course (Ottesen et al., 2014) were classified using the SVM-based classifier. As expected, retrieved *psbA* transcripts were most abundant in samples collected around mid-day and less abundant in samples collected around mid-night. After SVMs-based classification, most of the *psbA* sequences were identified as *Prochlorococcus*, including high light and low light ecotypes (54% and 12% on average respectively and subsequently merged in one category for downstream analysis) while only a minor fraction was classified as *Synechococcus psbA* (1% on average). The remaining sequences were classified as *Synechococcus* virus (27% on average) and *Prochlorococcus* virus (6% on average). Given that *Synechococcus* represents only a small fraction of the bacterioplankton in the time series of the North Pacific Subtropical Gyre (Ottesen et al., 2014), we hypothesized that the viral-*psbA* clustering into this group were not from *Synechococcus* viruses but instead from viruses that infect both *Prochlorococcus* and *Synechococcus*. Indeed, some cyanophages have shown to have a broad host range and infect strain from both genera (Sullivan et al., 2003). For example, the *psbA* found in the cyanophage P-SSM1, which was isolated using the *Prochlorococcus* strain MIT 9313 clustered with the *Synechococcus* virus group (Sullivan et al., 2006). Consequently, the two virus groups were redefined as Virus Group I (VG1; *Synechococcus* virus) and Virus Group II (VG2; *Prochlorococcus* virus). *Prochlorococcus* and *Synechococcus* are referred to in the figures respectively as Pro Bac and Syn Bac.

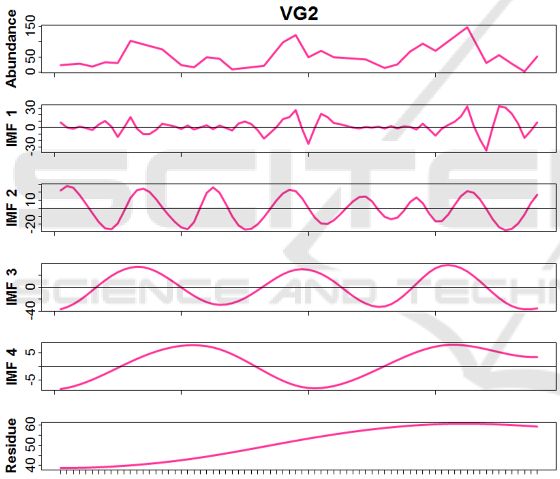

Figure 3: Empirical Mode Decomposition of Virus Group II (VG2) profile (*Prochlorococcus* virus).

PhoH sequences retrieved from the metatranscriptome did not show a change in abundance based on the time of the day (data not shown). The lack of variation for the *phoH* gene is probably due to the fact that light has a limited influence on the phosphate uptake. After SVMs-based classification, most *phoH* transcripts were assigned to heterotrophic phages (HP, 31% on average) and autotrophic bacteria host (A Host, 31% on average), followed by heterotrophic bacterial host (H Host, 21% on average) and autotrophic phages (AP, 14% on average). Few *phoH* sequences were classified as eukaryotic phytoplankton viruses (2% on average) in agreement with the notion that most of the primary production in the North Pacific Subtropical was supported by cyanobacteria. As a consequence, the *phoH* group including viruses infecting eukaryotic phytoplankton was removed from downstream analysis.

After classifying the sequences into their respective subgroups, we performed an empirical mode decomposition (EMD) (see Methods) on the transcriptional profiles of the subgroups, from which different diel patterns emerge within *psbA* and *phoH* transcripts. EMD decomposed each profile of classified AMGs into simpler harmonic waveforms or intrinsic mode functions (IMFs). While the EMD method lacks a formal procedure to associate a corresponding meaning/phenomena to each IMFs, complicating their interpretation in situations of total absence of knowledge about the system, in this case the underlying driving forces were not completely unknown. We identified a plausible biological explanation to each IMF to support our findings (in Figure 3 the complete EMD results for VG2 is shown as example). We hypothesize that the 1st order of IMFs captured most of the stochastic noise in each time series. The IMFs of the 3rd order could clearly identify a diel pattern in the expression of all AMGs (Figure 4), while the 2nd order IMF is able to detect what we believe are differences in the population heterogeneity among different groups (Figure 5).

SCITEPRESS SCIENCE AND TECHNOLOGY PUBLICATIONS

4.1 Diel Pattern Difference between Synechoccocus and Prochloroccocus

The IMFs of the 3rd order identified a diel pattern in the expression of all AMGs (Figure 4). The peak of expression of *psbA* from *Prochlorococcus* consistently occurred in the morning while a less-pronounced cycling of *Synechococcus psbA* transcripts occurred later in the afternoon (Figure 4A). This is consistent with a published dataset obtained using real-time PCR (Mella-Flores et al., 2012). The remarkable difference between the *psbA* expression levels of *Synechococcus* and *Prochlorococcus* is probably caused by the fact that *Prochlorococcus* is not able to withstand solar irradiance as high as *Synechococcus*. Consequently, as *Prochlorococcus* D1 protein is more sensitive to light, *psbA* needs to be highly expressed during the time of the day with the more irradiance (Mella-Flores et al., 2012).

Both VG1 and VG2 peaked during the daytime but the peak for VG2 was precisely matched to the peak in *Prochlorococcus psbA*. On the other hand, maximal expression of VG1 was more variable, possibly as a result of the variable proportions of the infected strains of *Prochlorococcus* and *Synechococcus* hosts. While transcripts from *psbA*-carrying virus had a very tight coupling to the time of the day, much less diel

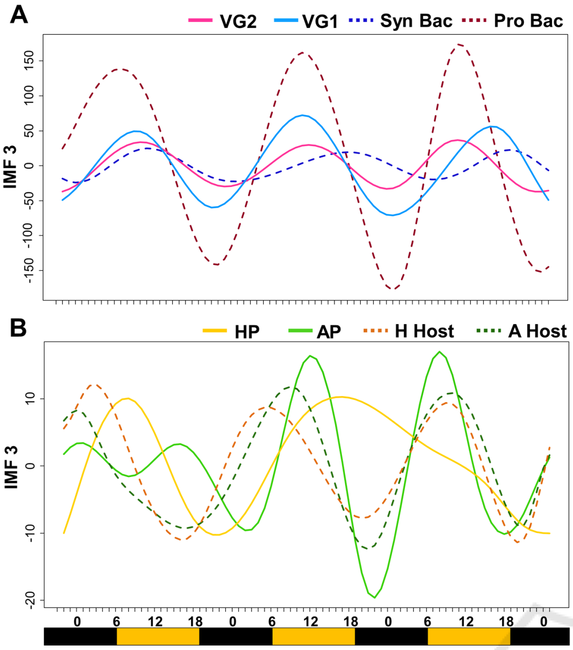

Figure 4: Intrinsic mode functions of 3rd order of *psbA* and *phoH* groups. X-Axis shows the time of the day, with the colored bar indicating the light-dark cycle. (A) *psbA* groups. (B) *phoH* groups.

effect was observed in *phoH* transcripts (Figure 4B) . VG1 and VG2 peaked at similar times as their hosts. On the contrary the HP transcripts consistently peaked later than the hosts homologs and, in general, the cycling of the *phoH* transcripts was less strong in tune with the daily light cycle.

4.2 The Population Structure Shows Different Viral Groups

Underlying the primary diel harmonics of the 3rd order IMF, the 2nd order was able to detect differences in the population heterogeneity among different groups. This was particularly evident during the final 30 hours of the time series, when a significant increase in temperature and salinity had been previously associated to a change in the transcriptional profile of SAR324 (Ottesen et al., 2014). Here, the shift in environmental conditions is detected as increased frequency in IMF2 for both *Prochlorococcus* and *Synechococcus* (Figure 5A), suggesting that the population heterogeneity of the 2 groups has expanded to include more ecotypes.

Differences in population heterogeneity are also observed as differences in IMF2 frequencies in VG1, VG2, AP and HP (Figure 5B). Interestingly the highest population heterogeneity (i.e. the highest IMF2 frequency) was observed in VG2, which also had the strongest correlation between AMG peak and the time of the day. Taken together, these observations suggest that VG2 includes many viral quasispecies with very narrow host ranges and a very precise control replication timing as a function of the time of the day and the low stability of the *Prochlorococcus*-type D1 protein. VG1 was less diverse but also appeared to have broader host range and the expression peak shifted in response to increased host diversity towards the end of the time-series.

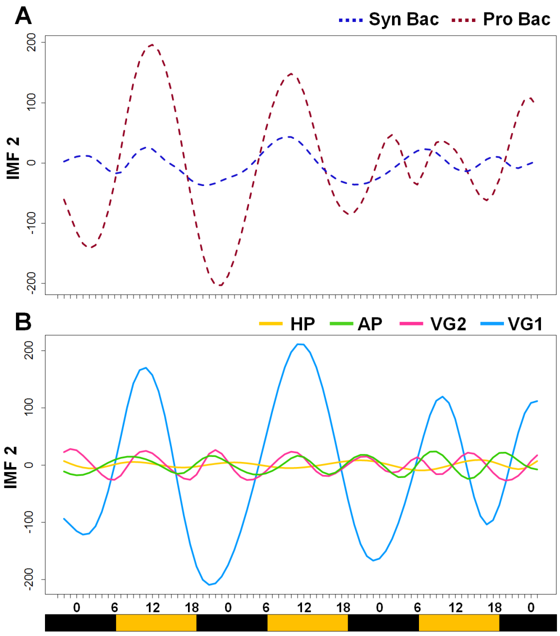

Figure 5: Intrinsic mode functions of 2nd order of *psbA* and *phoH* groups. X-Axis shows the time of the day, with the colored bar indicating the light-dark cycle. (A) population heterogeneity for Synechoccocus and Prochloroccocus groups. (B) Differences in population heterogeneity for all viral groups (both *psbA* and *phoH*).

The timing of the peak expression of the viral *psbA* also provided insights into the timing of cell lysis. Based on studies conducted in the laboratory, the viral *psbA* is transcribed at the end of the lytic cycle (Clokie et al., 2006b) and if replication of viral DNA is delayed until light, viral *psbA* expression should be minimal in the morning and slowly increase throughout the day.

Therefore, notwhitstanding the differences between VG1 and VG2, our findings are consistent with the hypothesis that most of the cell lysis and viral shedding occurs in the end of the day. Using SeaFlow cytometry which gives real-time continuous observations of cells abundance, Ribalet *et al.* (Ribalet et al., 2015) showed that *Prochlorococcus* cell numbers were higher in the day and sharply decrease at night, suggesting predation (viral and grazing) as the cause of the oscillation. Our data further support their

SCITEPRESS SCIENCE AND TECHNOLOGY PUBLICATIONS

hypothesis that viral infection might be a player in the synchronized oscillations of *Prochlorococcus* abundance from surface water of a Pacific Gyre (Ribalet et al., 2015).

5 CONCLUSIONS

Using a combination of SVMs based classification of short DNA sequences and EMD, we identified the existence of light-dark oscillations in the viral infection of cyanobacterial populations in the North Pacific Subtropical Gyre which can affect *Prochlorococcus* cell numbers and activity from surface water. Ottesen *et al.* (Ottesen et al., 2014) have observed diel cycling in the expression of genes from heterotrophic bacterioplankton and suggested that factors other than light might be linking the diel behaviours of autotrophs and heterotrophs.

Here we expand on that study to include cycling of expression of the viral assemblages and, based on the expression patterns of *psbA* and *phoH*, are able to identify major viral groups that differed in their response to light-dark cycles, population structure and their host range. Undoubtedly many other groups of cyanophages exist which do not carry those AMGs and which might or might not display circadian cycling, but a previous study suggests that as much as 88% of cyanophages do indeed carry a copy of the *psbA* gene (Sullivan et al., 2006). Because cyanophage ecotypes carrying similar AMGs are likely to occupy very similar ecological niches, it is conceivable that the existence of different replication patterns might allow coexistence of multiple ecotypes by suppressing competitive exclusion. We posit that cyanophages of the VG1-type overcome competititve exclusion with a broad host range and being able to initiate the replication cycle at different times of the day. On the other hand, the tight coupling between replication and lower stability of the *Prochlorococcus*-like D1 protein requires VG2 to have a much larger genetic diversity and a higher degree of specialization in host targets.

In addition to the ecological insights that this approach has provided in understanding cyanophage populations and their hosts, similar classification and decomposition analyses may be used to identify fundamental frequencies of natural processes from other time series data that otherwise would be overlooked.

ACKNOWLEDGEMENTS

The authors would like to acknowledge financial support from Singapores Ministry of Education Academic Research Fund Tier 3 under the research grant MOE2013-T3-1-013, Singapores National Research Foundation under its Marine Science Research and Development Programme (Award No. MSRDP-P13) and the Singapore Centre on Environmental Life Sciences Engineering (SCELSE), whose research is supported by the National Research Foundation Singapore, Ministry of Education, Nanyang Technological University and National University of Singapore, under its Research Centre of Excellence Program. The authors would like to thank Fabio Stella, Rohan Williams and James Houghton for their valuable feedbacks.

REFERENCES

Bagherzadeh, S. A. and Sabzehparvar, M. (2015). A local and online sifting process for the empirical mode decomposition and its application in aircraft damage detection. *Mechanical Systems and Signal Processing*, 54:68–83.

Breitbart, M., Thompson, L. R., Suttle, C. A., and Sullivan, M. (2007). Exploring the vast diversity of marine viruses. *Oceanography*, 20(SPL. ISS. 2):135–139.

Chambers, D. P. (2015). Evaluation of empirical mode decomposition for quantifying multi-decadal variations and acceleration in sea level records. *Nonlinear Processes in Geophysics*, 22(2):157–166.

Chang, C.-C. and Lin, C.-J. (2011). LIBSVM: A library for support vector machines. *ACM Transactions on Intelligent Systems and Technology*, 2:27:1–27:27.

Chang, K.-M. (2010). Ensemble empirical mode decomposition for high frequency ecg noise reduction. *Biomedizinische Technik/Biomedical Engineering*, 55(4):193–201.

Chen, C.-R., Shu, W.-Y., Chang, C.-W., and Hsu, I. C. (2014). Identification of under-detected periodicity in time-series microarray data by using empirical mode decomposition. *PloS one*, 9(11):e111719.

Chenard, C. and Suttle, C. A. (2008). Phylogenetic diversity of sequences of cyanophage photosynthetic gene psba in marine and freshwaters. *Applied and environmental microbiology*, 74(17):5317–5324.

Clokie, M. R., Millard, A. D., Mehta, J. Y., and Mann, N. H. (2006a). Virus isolation studies suggest short-term variations in abundance in natural cyanophage populations of the indian ocean. *Journal of the Marine Biological Association of the United Kingdom*, 86(03):499–505.

Clokie, M. R., Shan, J., Bailey, S., Jia, Y., Krisch, H. M., West, S., and Mann, N. H. (2006b). Transcription of a photosynthetict4-type phage during infection of a marine cyanobacterium. *Environmental Microbiology*, 8(5):827–835.

Golden, S. S., Ishiura, M., Johnson, C. H., and Kondo, T. (1997). Cyanobacterial circadian rhythms. *Annual review of plant biology*, 48(1):327–354.

Goldsmith, D. B., Crosti, G., Dwivedi, B., McDaniel, L. D., Varsani, A., Suttle, C. A., Weinbauer, M. G., Sandaa, R.-A., and Breitbart, M. (2011). Development of phoh as a novel signature gene for assessing marine phage diversity. *Applied and environmental microbiology*, 77(21):7730–7739.

Goldsmith, D. B., Parsons, R. J., Beyene, D., Salamon, P., and Breitbart, M. (2015). Deep sequencing of the viral phoh gene reveals temporal variation, depth-specific composition, and persistent dominance of the same viral phoh genes in the sargasso sea. *PeerJ*, 3:e997.

Han, J. and van der Baan, M. (2013). Empirical mode decomposition for seismic time-frequency analysis. *Geophysics*, 78(2):O9–O19.

Hess, W. R. (2004). Genome analysis of marine photosynthetic microbes and their global role. *Current opinion in biotechnology*, 15(3):191–198.

Huang, N. E., Shen, Z., Long, S. R., Wu, M. C., Shih, H. H., Zheng, Q., Yen, N.-C., Tung, C. C., and Liu, H. H. (1998). The empirical mode decomposition and the hilbert spectrum for nonlinear and non-stationary time series analysis. In *Proceedings of the Royal Society of London A: Mathematical, Physical and Engineering Sciences*, volume 454, pages 903–995. The Royal Society.

Kim, D. and Oh, H.-S. (2009). Emd: a package for empirical mode decomposition and hilbert spectrum. *The R Journal*, 1(1):40–46.

Li, F., Jo, Y.-H., Liu, W. T., and Yan, X.-H. (2012). A dipole pattern of the sea surface height anomaly in the north atlantic: 1990s–2000s. *Geophysical Research Letters*, 39(15).

Lindell, D., Jaffe, J. D., Coleman, M. L., Futschik, M. E., Axmann, I. M., Rector, T., Kettler, G., Sullivan, M. B., Steen, R., Hess, W. R., et al. (2007). Genome-wide expression dynamics of a marine virus and host reveal features of co-evolution. *Nature*, 449(7158):83–86.

Mella-Flores, D., Six, C., Ratin, M., Partensky, F., Boutte, C., Le Corguillé, G., Marie, D., Blot, N., Gourvil, P., Kolowrat, C., et al. (2012). Prochlorococcus and synechococcus have evolved different adaptive mechanisms to cope with light and uv stress.

Ni, T. and Zeng, Q. (2016). Diel infection of cyanobacteria by cyanophages. *Frontiers in Marine Science*, 2:123.

Ottesen, E. A., Young, C. R., Gifford, S. M., Eppley, J. M., Marin, R., Schuster, S. C., Scholin, C. A., and DeLong, E. F. (2014). Multispecies diel transcriptional oscillations in open ocean heterotrophic bacterial assemblages. *Science*, 345(6193):207–212.

Partensky, F., Hess, W. R., and Vaulot, D. (1999). Prochlorococcus, a marine photosynthetic prokaryote of global significance. *Microbiology and molecular biology reviews*, 63(1):106–127.

Paulson, J. N., Stine, O. C., Bravo, H. C., and Pop, M. (2013). Differential abundance analysis for microbial marker-gene surveys. *Nature methods*, 10(12):1200–1202.

Ribalet, F., Swalwell, J., Clayton, S., Jiménez, V., Sudek, S., Lin, Y., Johnson, Z. I., Worden, A. Z., and Armbrust, E. V. (2015). Light-driven synchrony of prochlorococcus growth and mortality in the subtropical pacific gyre. *Proceedings of the National Academy of Sciences*, 112(26):8008–8012.

Sandberg, R., Winberg, G., Bränden, C.-I., Kaske, A., Ernberg, I., and Cöster, J. (2001). Capturing whole-genome characteristics in short sequences using a naive bayesian classifier. *Genome research*, 11(8):1404–1409.

Stitson, M., Weston, J., Gammerman, A., Vovk, V., and Vapnik, V. (1996). Theory of support vector machines. *Technical Report, CSD-TR-96–17, Computational Intelligence Group, University of London*.

Sullivan, M. B., Lindell, D., Lee, J. A., Thompson, L. R., Bielawski, J. P., and Chisholm, S. W. (2006). Prevalence and evolution of core photosystem ii genes in marine cyanobacterial viruses and their hosts. *PLoS Biol*, 4(8):e234.

Sullivan, M. B., Waterbury, J. B., and Chisholm, S. W. (2003). Cyanophages infecting the oceanic cyanobacterium prochlorococcus. *Nature*, 424(6952):1047–1051.

Suttle, C. A. and Chen, F. (1992). Mechanisms and rates of decay of marine viruses in seawater. *Applied and Environmental Microbiology*, 58(11):3721–3729.

Thompson, L. R., Zeng, Q., Kelly, L., Huang, K. H., Singer, A. U., Stubbe, J., and Chisholm, S. W. (2011). Phage auxiliary metabolic genes and the redirection of cyanobacterial host carbon metabolism. *Proceedings of the National Academy of Sciences*, 108(39):E757–E764.

Tzahor, S., Man-Aharonovich, D., Kirkup, B. C., Yogev, T., Berman-Frank, I., Polz, M. F., Béjà, O., and Mandel-Gutfreund, Y. (2009). A supervised learning approach for taxonomic classification of core-photosystem-ii genes and transcripts in the marine environment. *BMC genomics*, 10(1):229.

Wilhelm, S. W., Weinbauer, M. G., Suttle, C. A., and Jeffrey, W. H. (1998). The role of sunlight in the removal and repair of viruses in the sea. *Limnology and Oceanography*, 43(4):586–592.

Zhao, Y., Tang, H., and Ye, Y. (2011). Rapsearch2: a fast and memory-efficient protein similarity search tool for next-generation sequencing data. *Bioinformatics*, 28(1):125–126.